Model. Earth Syst. Environ. (2016) 2:112
DOI 10.1007/s40808-016-0168-9

ORIGINAL ARTICLE

Fate of dissolved oxygen and survival of fish population in aquatic ecosystem with nutrient loading: a model

O. P. Misra[1] · **Divya Chaturvedi**[2]

Received: 30 April 2016 / Accepted: 4 June 2016 / Published online: 21 June 2016

Abstract In this paper, a nonlinear mathematical model is proposed and analyzed to study the depletion of dissolved oxygen and survival or extinction of fish population in a nutrient enriched aquatic ecosystem. It is assumed in the model that there is an external constant input of nutrients (phosphorus and nitrogen) in the water body on account of anthropogenic activities. Stability analysis of the equilibria of the model is carried out and from the analysis it is shown that the fish population will survive at very low equilibrium level due to reduced concentration of dissolved oxygen and excessive presence of algal biomass on account of nutrient loading. Further, it is shown in this paper that the fish population tend to extinction due to decrease in the concentration of dissolved oxygen from its threshold level. Numerical simulations are also carried out in this paper to support the analytical results.

Keywords Fish · Dissolved oxygen · Nutrients · Algae · Stability · Equilibria

Introduction

Phosphorus and nitrogen are the primary nutrients that in excessive amounts pollute our aquatic ecosystem. Human related activities can accelerate the rate at which nutrients enter the aquatic ecosystem. Nitrogen and phosphorus support the growth of algae and aquatic plants which provide food and habitat for fish, shellfish and smaller organisms that live in water. But, too much nitrogen and phosphorus that enter into the water due to human activities causes algae to grow faster than ecosystems can handle. Significant increase in algae harm water quality, food resources and habitats, and decreases the oxygen that fish and other aquatic life need to survive. Large growths of algae are called algal blooms and they can severely reduce or eliminate oxygen in the water, leading to illnesses in fish and death of large number of fishes. Hypoxia or oxygen depletion is a phenomenon that occurs in aquatic environments as dissolved oxygen becomes reduced in concentration to a point detrimental to aquatic organisms living in the system and it is observed that fish cannot live below 30 % dissolved oxygen saturation. When the oxygen level is maintained near saturation or even at slightly super saturation at all times it will increase growth rates, reduce the food conversion ratio and increase overall fish production. Smith and Piedrahita (1988) in their paper have studied the relationship between algal biomass and dissolved oxygen dynamics and shown that dissolved oxygen levels would be greatly improved if algal biomass could be maintained at intermediate levels. Associated with the dominance of cyanobacteria (blue-green algae) are several negative effects, such as reduced transparency, decreased biodiversity, elevated primary production and the potential occurrence of oxygen depletion which may result in massive fish kills (Reynolds 1991). Empirical relationships were developed between algal bloom frequencies and total phosphorus concentrations for three distinct regions of Lake Okeechobee, and hypotheses were derived to explain observed spatial variation in those relationships. When phosphorus concentrations were between 30 and 60 μg L^{-1}

✉ Divya Chaturvedi
chaturvedi.divya14@gmail.com

O. P. Misra
misra_op@rediffmail.com

[1] School of Mathematics and Allied Sciences, Jiwaji University, Gwalior, MP, India

[2] School of Mathematics and Allied Sciences, Jiwaji University, Gwalior, MP, India

in the littoral regions, frequency or risk of an algal bloom increased with phosphorus concentration. The maximum risk of an algal bloom generally occurred when phosphorus exceeded 60 μg L^{-1}. This condition was observed 70 % of the time in the open lake, 29 % of the time in the north littoral, and 15 % of the time in the south littoral. When phosphorus concentration exceeded 60 μg L^{-1}, risk of 40 μg L^{-1} bloom was 19 % in the open lake, 28 % in the north littoral, and 60 % in the south littoral (Walker and Havens 1995). On a global basis, strong correlations have been demonstrated between total phosphorus inputs and phytoplankton production in fresh waters, and between total nitrogen input and phytoplankton production in estuarine and marine waters. There are also numerous examples in geographic regions ranging from the largest and second largest US mainland estuaries (Chesapeake Bay and the Albemarle-Pamlico Estuarine System), to the Inland Sea of Japan, the Black Sea, and Chinese coastal waters, where increase in nutrient loading have been linked with the development of large biomass blooms, leading to anoxia and even toxic or harmful impacts on fisheries resources, ecosystems, and human health or recreation (Anderson et al. 2002). Extensive kills of both invertebrates and fishes are probably the most dramatic manifestation of hypoxia (or anoxia) in eutrophic and hypereutrophic aquatic ecosystems with low water turnover rates (Camargo and Alonso 2006).

Dynamics of nutrient driven phytoplankton blooms has been studied by Huppert et al. (2002) with the help of mathematical model. A real-time three dimensional model for eutrophication, based upon the numerically generated boundary-fitted orthogonal curvilinear grid system with a grid block technique and integrated with the prediction of hydrodynamic variables simultaneously, has been implemented by Chau (2004). The model simulates the transport and transformation of nine water quality constituents associated with eutrophication in the waters, including Chl-a, DO, CBOD, organic nitrogen, NH_4-N, $NO_2 + -NO_3$-N, organic phosphorus, PO_4-P, and zooplankton. Author in this paper has made comparison of computational results with measured data available in Tolo Harbour which demonstrates its capability to mimic the algal growth dynamics and water quality process reasonably. In the next paper (Huppert et al. 2005) proposed and analysed a mathematical model to study the dynamics of seasonally recurring algae blooms considering a generic bottom-up nutrient phytoplankton system. Misra et al. (2006) investigated a nonlinear mathematical model to study the depletion of dissolved oxygen due to discharge of organic pollutants in a water body by considering biodegradation and biochemical processes in the food chain involving bacteria, protozoa, and an aquatic population. It is shown in this paper that if organic pollutants are continuously discharged into water body, the concentration of dissolved oxygen may become negligibly small, which may consequently threaten the survival of aquatic populations. A nonlinear mathematical model is proposed by Shukla et al. (2007) to study the depletion of dissolved oxygen in water body caused by industrial and household discharges of organic matters (pollutants). The effect of depleted level of dissolved oxygen on the survival of biological species in such an aquatic ecosystem is also studied in this paper using mathematical model. Using stability theory authors have shown that not only the concentration of dissolved oxygen decreases due to various biodegradation and biochemical processes but also the survival of biological species is threatened. In this paper it has been also shown that if the organic pollutants continue to be discharged into the water body, the concentration of dissolved oxygen may become negligibly small and the biological species wholly dependent on it may tend to extinction. Shukla et al. (2008) studied a mathematical model to investigate the simultaneous effect of water pollution and eutrophication on the concentration of dissolved oxygen (DO) in a water body. With the help of mathematical model (Alvarez-Vazquez et al. 2009) have studied the interactions of nutrients, phytoplankton, zooplankton, organic detritus, and dissolved oxygen in an aquatic media which is under eutrophication process. Chen et al. (2009) in their paper have presented a mathematical model to describe how nitrogen and phosphorus affect the bloom, persistence, and extinction of blue-green algae in lakes. Misra (2011) proposed a mathematical model to study the depletion of dissolved oxygen in a lake caused by algal bloom by considering Holling type-III interaction between nutrients and algal population. From the analysis of the model author has shown that the continuous supply of nutrients lead to algal bloom in the lake and consequently decrease the concentration of dissolved oxygen. Author has also shown that if the conversion rate of detritus into nutrients increases then the density of algal bloom increases whereas the concentration of dissolved oxygen decreases. Chakraborty and Das (2015) have analyzed a mathematical model to investigate the effects of toxic substances released by external agents into natural system consisting of one-phytoplankton and two-zooplankton species system with harvesting. Chakraborty et al. (2015) studied the spatial dynamics of a nutrient-phytoplankton system with toxic effect on phytoplankton and have shown that the distribution of nutrients and phytoplankton exhibits spatio temporal oscillation for certain level of toxicity. It is noted here that in all these mathematical models authors have not considered the role of algal biomass on reaeration coefficient and carrying capacity of the environment while studying the dynamics of aquatic ecosystem

comprising of dissolved oxygen, nutrients, algal biomass and fish population.

Therefore, in view of the above in this paper we have proposed and analyzed a nonlinear mathematical model to study the survival of fish population in an aquatic ecosystem considering the effect of algal biomass on reaeration process and also on carrying capacity of aquatic environment which is assumed to be deficient in dissolved oxygen due to excessive growth of algal biomass caused by nutrient (phosphorus and nitrogen) overloading.

Mathematical model

We consider an aquatic ecosystem in which nutrients (phosphorus and nitrogen) are continuously discharged due to anthropogenic activities such as runoff from agriculture and development, pollution from septic systems and sewers, sewage sludge spreading, etc.

Let F and C denote the density of fish population and concentration of dissolved oxygen in water bodies respectively. P denotes the concentration of nutrients (phosphorus and nitrogen) and N represents the algal biomass.

Keeping in view the above considerations the mathematical model describing the system is given by the following set of differential equations:

$$\frac{dF}{dt} = R(C)F - \frac{r_0F^2}{K(N)}, \tag{1}$$

$$\frac{dC}{dt} = -d_{B0} + d_{B1}(N_0 - N) + K_2(N)(C_s - C), \tag{2}$$

$$\frac{dP}{dt} = I - rP - \frac{d_1PN}{b+P} + \beta_1 aN, \tag{3}$$

$$\frac{dN}{dt} = \frac{d_1PN}{b+P} - aN - gN^2, \tag{4}$$

with the initial conditions as:

$C(0) = H_0 > 0, \quad F(0) = F_0 > 0, \quad N(0) = A_0 > 0, P(0) = P_0 > 0.$

In the present analysis we assume the following forms for functions

$R(C) = r_0 + r_1(C - C_0); \quad K(N) = K_0 - K_{11}N; K_2(N) = \frac{K_{20}}{1+N}; \quad C \le C_s.$

The function $R(C)$ denotes the growth rate of fish population which depends upon dissolved oxygen and is assumed to be an increasing function of dissolved oxygen. In an aquatic system, oxygen is available in water in dissolved form, known as dissolved oxygen (DO). Most of the aquatic populations e.g. fish etc. are wholly dependent on dissolved oxygen (DO) for breathing and it is observed that in many aquatic bodies massive death of fish population has occured due to low level of dissolved oxygen (DO). The function $K(N)$ denotes the carrying capacity of fish population which is assumed to be decreasing function of algal biomass. Reaeration coefficient $K_2(N)$ also depends upon algal biomass and decreases as algal biomass increases. The over growth of algal population is known as algal bloom, which may cause eutrophication. Algae grow very fast at high nutrient concentrations and may cover the whole surface of the lake. The dissolved oxygen (DO) is being produced in the lake by surface re-aeration which includes the transfer of atmospheric oxygen to the lake. When surface area of the water is being covered by the floating algae, then the transfer of oxygen from air to water is reduced.

r_0 is the intrinsic growth rate of fish, r_1 is control parameter for the growth of fish population depending upon level of dissolved oxygen, C_0 is the threshold level of concentration of dissolved oxygen, K_0 is natural carrying capacity, K_{11} is reduction rate in carrying capacity due to algal biomass, d_{B0} is natural depletion rate of dissolved oxygen, N_0 is threshold level of algal biomass and it is assumed that when N is more than the threshold level N_0 then the concentration of dissolved oxygen will decrease because when algae die and sink to the bottom of the water body detritus is formed and detritus while decaying uses dissolved oxygen and hence reducing the concentration of dissolved oxygen in aquatic body but when N is less than the threshold level N_0 then the concentration of dissolved oxygen will increase because dissolved oxygen is produced as a product of photosynthesis from phytoplankton algae, seaweed and other aquatic plants, d_{B1} is the growth rate coefficient of dissolved oxygen depending upon the level of algal biomass, K_{20} is natural reaeration rate, C_s is saturated concentration of dissolved oxygen, I is the input rate of nutrients (phosphorus,nitrogen), r is the depletion rate of nutrients (phosphorus, nitrogen), β_1 is nutrients (phosphorus, nitrogen) recycling coefficient. The nutrients are also being supplied by detritus, which is being formed from the dead part of the algal population, a is depletion rate of algal biomass, g is depletion rate of algal biomass due to crowding. The term $\frac{d_1PN}{b+P}$ represents the growth of algal biomass due to nutrients present in the water body, d_1 is the maximum specific growth rate of algae population, b is half saturation constant. Here, all the parameters $K_0, K_{11}, K_{20}, r_0, r_1, d_{B0}, d_{B1}, N_0, I, r, d_1, b, \beta_1, a, g$ are taken to be positive constants.

Equilibria of the model

The system of Eqs. (1–4) has following four feasible equilibria:

1. *Boundary equilibrium point* E_1:-

$E_1 = (F^*, C^*, P^*, N^*)$,
where $F^* = 0$, $C^* = \frac{-d_{B0}+d_{B1}N_0}{K_{20}} + C_s$, $P^* = \frac{I}{r}$, $N^* = 0$ and $C^* > 0$ if $C_sK_{20} + d_{B1}N_0 > d_{B0}$ holds good.

2. *Boundary equilibrium point* E_2:-

$E_2 = (\hat{F}, \hat{C}, \hat{P}, \hat{N})$,
where $\hat{F} = \frac{\{r_0+r_1(\hat{C}-C_0)\}(K_0)}{r_0}$, $\hat{C} = C_s + \frac{d_{B1}N_0}{K_{20}} - \frac{d_{B0}}{K_{20}}$,, $\hat{C} > 0$ and $\hat{F} > 0$ provided the conditions $C_sK_{20} + d_{B1}N_0 > d_{B0}$ and $\hat{C} > C_0$ are satisfied. $\hat{P} = \frac{I}{r}$, $\hat{N} = 0$.

3. *Boundary equilibrium point* E_3:-

$E_3 = (\tilde{F}, \tilde{C}, \tilde{P}, \tilde{N})$,
where $\tilde{F} = 0$, $\tilde{C} = C_s + \frac{(d_{B1}(N_0-\tilde{N})-d_{B0})(1+\tilde{N})}{K_{20}}$ and $\tilde{C} > 0$ and if $C_sK_{20} + d_{B1}N_0(1+\tilde{N}) > (d_{B0} + d_{B1}\tilde{N})(1+\tilde{N})$ is satisfied.
$\tilde{N} = \frac{1}{g}\left(\frac{d_1\tilde{P}}{b+\tilde{P}} - a\right)$ and $\tilde{N} > 0$ provided $(d_1 - a)\tilde{P} > ab$ holds good.
$\tilde{P}$ is given by the positive root of the following equation:

$$rg\tilde{P}^3 + \tilde{P}^2(d_1^2 - ad_1(1+\beta_1) + a^2\beta_1 + 2rgb - Ig) + \tilde{P}(2a^2b\beta_1 - ad_1\beta_1 b - abd_1 - 2bIg + rgb^2) - (Igb^2 - a^2b^2\beta_1) = 0 \quad (5)$$

According to Descartes' rule of sign the above polynomial given by Eq. (5) is of third degree and will have at least one positive root if the following conditions are satisfied:
$d_1^2 + a^2\beta_1 + 2rgb < ad_1(1+\beta_1) + Ig, 2a^2\beta_1 + rgb < ad_1(1+\beta_1) + 2Ig$ and $Ig > a^2\beta_1$.

4. *Interior equilibrium point* E_4:-

$E_4 = (\bar{F}, \bar{C}, \bar{P}, \bar{N})$, where, $\bar{F} = \frac{(r_0+r_1(\bar{C}-C_0))K(\bar{N})}{r_0}$ and $\bar{F} > 0$ provided the conditions $K_0 > K_{11}\bar{N}, C_sK_{20} + d_{B1}N_0(1+\bar{N}) > d_{B0}(1+\bar{N}) + C_0K_{20} + d_{B1}\bar{N}\ (1+\bar{N})$ are satisfied.
$\bar{C} = C_s + \frac{(d_{B1}(N_0-\bar{N})-d_{B0})(1+\bar{N})}{K_{20}}$
and $\bar{C} > 0$ if $C_sK_{20} + d_{B1}N_0(1+\bar{N}) > (d_{B0} + d_{B1}\bar{N})(1+\bar{N})$ holds good. $\bar{N} = \frac{1}{g}\left(\frac{d_1\bar{P}}{b+\bar{P}} - a\right)$ and $\bar{N} > 0$ if $(d_1 - a)\bar{P} > ab$ should hold good.
$\bar{P}$ is given by the positive root of the following equation:

$$rg\bar{P}^3 + \bar{P}^2(d_1^2 - ad_1(1+\beta_1) + a^2\beta_1 + 2rgb - Ig) + \bar{P}(2a^2b\beta_1 - ad_1\beta_1 b - abd_1 - 2bIg + rgb^2) - (Igb^2 - a^2b^2\beta_1) = 0 \quad (6)$$

The above polynomial given by Eq. (6) is of third degree and will have atleast one positive root if the following conditions are satisfied: $d_1^2 + a^2\beta_1 + 2rgb < ad_1(1+\beta_1) + Ig, 2a^2\beta_1 + rgb < ad_1(1+\beta_1) + 2Ig$ and $Ig > a^2\beta_1$.

Remark 1 From second boundary equilibrium point E_2, we have

$\hat{F} = \frac{\{r_0+r_1(\hat{C}-C_0)\}(K_0)}{r_0}$ and it may be noted that the fish population will exist if the equilibrium concentration of dissolved oxygen is more than its threshold level.
On differentiating $\hat{F}$ with respect to $\hat{C}$, we find that $\frac{\partial\hat{F}}{\partial\hat{C}} = \frac{r_1K_0}{r_0} > 0$.
From the positivity of $\frac{\partial\hat{F}}{\partial\hat{C}}$, it may be noted that as the equilibrium concentration of dissolved oxygen increases then the equilibrium level of fish population also increases.

Remark 2 From third boundary equilibrium point E_3, we find that

$\tilde{C} = C_s + \frac{(d_{B1}(N_0-\tilde{N})-d_{B0})(1+\tilde{N})}{K_{20}}$ and $\tilde{N} = \frac{1}{g}\left(\frac{d_1\tilde{P}}{b+\tilde{P}} - a\right)$.
On differentiating $\tilde{C}$ with respect to $\tilde{N}$, we obtain, $\frac{\partial\tilde{C}}{\partial\tilde{N}} = \frac{d_{B1}(N_0-2\tilde{N}-1)-d_{B0}}{K_{20}} < 0$ if $N_0 < 2\tilde{N} + 1$.
It is noted here that if natural level of algal biomass is less than the sum of twice of equilibrium level of algal biomass and one then the equilibrium concentration of dissolved oxygen decreases as the equilibrium level of algal biomass increases.
On differentiating $\tilde{N}$ with respect to $\tilde{P}$, we find that $\frac{\partial\tilde{N}}{\partial\tilde{P}} = \frac{bd_1}{g(b+\tilde{P})^2} > 0$.
It is noted here that as the equilibrium concentration of nutrients increases then the equilibrium level of algal biomass also increases. This shows that the nutrients play an important role in algal growth.

Remark 3 From interior equilibrium point E_4, we see that

$\bar{F} = \frac{(r_0+r_1(\bar{C}-C_0)K(\bar{N})}{r_0}$
and on differentiating $\bar{F}$ with respect to $\bar{N}$, we obtain $\frac{\partial\bar{F}}{\partial\bar{N}} = \frac{-K_{11}(r_0+r_1(\bar{C}-C_0))}{r_0} + \frac{r_1K(\bar{N})(-d_{B1}(1+2\bar{N}-N_0)-d_{B0})}{r_0K_{20}} < 0$ provided $\bar{C} > C_0$, $N_0 < 2\bar{N} + 1$ and $K(\bar{N}) > 0$.
This shows that as the equilibrium level of algal biomass increases then the equilibrium fish population reduces but will exist at low equilibrium provided the

equilibrium concentration of dissolved oxygen exceeds its threshold value.

On differentiating $\bar{F}$ with respect to $\bar{C}$, we find that $\frac{\partial \bar{F}}{\partial \bar{C}} = \frac{(K_0 - K_{11}\bar{N})r_1}{r_0} > 0$ if $K(\bar{N}) > 0$.

Thus, when the carrying capacity is positive then from the positivity of $\frac{\partial \bar{F}}{\partial \bar{C}}$, it is clear that as the equilibrium concentration of dissolved oxygen increases then the equilibrium fish population also increases. $\bar{C} = C_s + \frac{(d_{B1}(N_0 - \bar{N}) - d_{B0})(1+\bar{N})}{K_{20}}$.

On differentiating $\bar{C}$ with respect to $\bar{N}$, we find that $\frac{\partial \bar{C}}{\partial \bar{N}} = \frac{d_{B1}(N_0 - 2\bar{N} - 1) - d_{B0}}{K_{20}} < 0$ provided $N_0 < 2\bar{N} + 1$.

Hence, it is noted that if natural level of algal biomass is less than the sum of twice of equilibrium level of algal biomass and one then the equilibrium concentration of dissolved oxygen decreases as the equilibrium level of algal biomass increases.

$\bar{N} = \frac{1}{g}\left(\frac{d_1 \bar{P}}{b+\bar{P}} - a\right)$.

On differentiating $\bar{N}$ with respect to $\bar{P}$, we obtain that $\frac{\partial \bar{N}}{\partial \bar{P}} = \frac{bd_1}{g(b+\bar{P})^2} > 0$.

It is noted from the above expression that as the equilibrium concentration of nutrients increases then the equilibrium level of algal biomass also increases.

Positivity of solutions

Model describes the effect of nutrient loading on concentration of dissolved oxygen and fish population in an aquatic ecosystem, therefore it is very important to show that all variables will be positive for all time. Positivity implies that the system persists. For positivity of solutions we have to show that the solution ($F(t)$, $C(t)$, $P(t)$, $N(t)$) of the system given by Eqs. (1–4) with positive initial conditions $C(0) = H_0 > 0, F(0) = F_0 > 0$,

$N(0) = A_0 > 0, P(0) = P_0 > 0$ are positive for all $t > 0$.

From Eq. (1) of the system, we get

$$\frac{dF}{dt} \geq -\left(r_1 C_0 + \frac{r_0 F_u}{K_0 - K_{11}N_u}\right)F.$$

On solving above differential inequality we obtain

$$F \geq F_0 exp\left\{-\left(\frac{r_0 F_u t}{K_0 - K_{11}N_u} + r_1 C_0\right)t\right\}.$$

Hence, we find that $F > 0$ as $t \to \infty$.

From Eq. (2) of the system, we get

$$\frac{dC}{dt} \geq -\left(d_{B0} + d_{B1}N_u - \frac{K_{20}C_s}{1+N_u} + K_{20}C\right).$$

On solving above differential inequality we obtain

$$C \geq \left(-d_{B0} - d_{B1}N_u + \frac{K_{20}C_s}{1+N_u}\right)\frac{1}{K_{20}} + \left(H_0 - \left(-d_{B0} - d_{B1}N_u + \frac{K_{20}C_s}{1+N_u}\right)\frac{1}{K_{20}}\right)exp(-K_{20}t).$$

Thus, we find that $C > 0$ as $t \to \infty$ provided

$$\frac{K_{20}C_s}{1+N_u} > d_{B0} + d_{B1}N_u.$$

From Eq. (3) of the system, we get

$$\frac{dP}{dt} \geq (I - rP - d_1 N_u).$$

On solving above differential inequality we obtain

$$P \geq \frac{I - d_1 N_u}{r} + \left(P_0 - \left(\frac{I - d_1 N_u}{r}\right)\right)exp(-rt).$$

Therefore, it is observed that $P > 0$ as $t \to \infty$ provided

$$I > d_1 N_u.$$

From Eq. (4) of the system, we have

$$\frac{dN}{dt} \geq -(a + gN_u)N.$$

On solving above differential inequality we obtain

$$N \geq A_0 exp\{-(a + gN_u)t\}.$$

Hence, we see that $N > 0$ as $t \to \infty$.

Boundedness of the system

In this section, we will establish that the system described by Eqs. (1–4) is bounded. In the following lemma we have shown that all the solutions are bounded in the region H_1.

Lemma 1 *All the solutions of model will lie in the region* $H_1 = \{(F, C, P, N) \in R_+^4 : 0 \leq F \leq F_u, 0 \leq C \leq C_u, 0 \leq P_l \leq P \leq P_u, 0 \leq N_l \leq N \leq N_u\}$, *as* $t \to \infty$, *for all positive initial values* $(F(0), C(0), P(0), N(0)) \in H_1 \subset R_+^4$

Proof From Eq. (4) of the model we have:

$$\frac{dN}{dt} \leq N(d_1 - a - gN),$$

$$\frac{dN}{dt} \leq N(w - gN),$$

where, $w = (d_1 - a) > 0$.

Then, by usual comparison theorem (Hale 1969), we get as $t \to \infty$:

$$\limsup_{t \to \infty} N(t) \leq \frac{d_1 - a}{g} = N_u. \quad (7)$$

From Eq. (3) of the model we have:

$$\frac{dP}{dt} \leq I - rP + \beta_1 a N_u,$$

$$\frac{dP}{dt} + rP \leq I + \beta_1 a N_u.$$

Then, by usual comparison theorem (Hale 1969), we get as $t \to \infty$:

$$\limsup_{t\to\infty} P(t) \leq \frac{I + \beta_1 a N_u}{r} = P_u. \tag{8}$$

From Eq. (2) of the model we have:

$$\frac{dC}{dt} \leq d_{B1} N_0 + K_{20} C_s - \frac{K_{20}}{1 + N_u} C,$$

$$\frac{dC}{dt} + \frac{K_{20}}{1 + N_u} C \leq d_{B1} N_0 + K_{20} C_s.$$

Then by usual comparison theorem (Hale 1969), we get as $t \to \infty$:

$$\limsup_{t\to\infty} C(t) \leq \frac{(d_{B1} N_0 + K_{20} C_s)(1 + N_u)}{K_{20}} = C_u. \tag{9}$$

Now from Eq. (1) of the model we have:

$$\frac{dF}{dt} \leq F r_0 + r_1 C_u F - \frac{r_0 F^2}{K_0}.$$

Let $r_0 + r_1 C_u = M$, then

$$\frac{dF}{F(M - \frac{r_0 F}{K_0})} \leq dt.$$

Then by usual comparison theorem (Hale 1969), we get as $t \to \infty$:

$$\limsup_{t\to\infty} F(t) \leq \frac{M K_0}{r_0} = F_u. \tag{10}$$

Again, from Eq. (3) of the model we have:

$$\frac{dP}{dt} \geq I - rP - \frac{d_1 P N_u}{b + P},$$

$$\frac{dP}{dt} + P\left(r + \frac{d_1 N_u}{b}\right) \geq I.$$

Then, by usual comparison theorem (Hale 1969), we get as $t \to \infty$:

$$\liminf_{t\to\infty} P(t) \geq \frac{Ib}{rb + d_1 N_u} = P_l. \tag{11}$$

Now, from Eq. (4) of the model we have:

$$\frac{dN}{dt} \geq N\left(\frac{d_1 P_l}{b + P_l} - a - gN\right),$$

$$\frac{dN}{dt} \geq N(Z_1 - gN).$$

Let

$$Z_1 = \frac{d_1 P_l}{b + P_l} - a > 0,$$

$$\frac{dN}{N(Z_1 - gN)} \geq dt.$$

Then, by usual comparison theorem (Hale 1969), we get as $t \to \infty$:

$$\liminf_{t\to\infty} N(t) \geq \frac{1}{g}\left(\frac{d_1 P_l}{b + P_l} - a\right) = N_l. \tag{12}$$

Since,

$$\frac{d_1 P_l}{b + P_l} - a > 0.$$

Hence, we get

$$\frac{Ib}{rb + d_1 N_u} > \frac{ab}{d_1 - a}. \tag{13}$$

This completes the proof of the lemma. □

Theorem 1 *The Box H_1 is a compact positively invariant set in space FCPN.*

Proof Consider the system comprising of Eqs. (1–4). To prove the theorem, we consider a point $D_1 = (F', C', P', N')$ outside the box H_1, with $F' > F_u, C'_u$, $P' > P_u$, and $N' > N_u$ and take the box H_1 in the phase space *FCPN* with one vertex located at the origin and other at D_1. Now, let us compute the angle that the flow makes with each one of the faces of H_1 not lying on the coordinate planes. Consider the planes $\pi_F : F = F', \pi_C : C = C', \pi_P : P = P', \pi_N : N = N'$ and let n_F, n_C, n_P, n_N are outward unit normal vectors (with respect to box H_1) respectively to each plane. Then

$$n_F \frac{dD_1}{dt}\Big|_{\pi_F} = F'[r_0 + r_1(C - C_0)] - \frac{r_0 F'^2}{K(N)},$$

$$n_F \frac{dD_1}{dt}\Big|_{\pi_F} \leq F'\left(r_0 + r_1 C_u - \frac{r_0 F'}{K_0}\right) - r_1 C_0 F'.$$

Since,

$$F' > \frac{(r_0 + r_1 C_u) K_0}{r_0},$$

therefore we get,

$$n_F \frac{dD_1}{dt}\Big|_{\pi_F} \leq -r_1 C_0 F',$$

hence,

$$n_F \frac{dD_1}{dt}\Big|_{\pi_F} \leq 0.$$

Similarly we can show that,

$$n_C \frac{dD_1}{dt}|_{\pi_C} \leq 0, n_P \frac{dD_1}{dt}|_{\pi_P} \leq 0, n_N \frac{dD_1}{dt}|_{\pi_N} \leq 0,$$

where,

$$\frac{dD_1}{dt} = \left(\frac{dF}{dt}, \frac{dC}{dt}, \frac{dP}{dt}, \frac{dN}{dt}\right).$$

Thus, the flow along the normal to each of the plane is again moving towards the box. Therefore we can say that box H_1 is a compact positively invariant box. This completes the proof of the theorem.

Now, it is clear from the above theorem that the trajectories of the system cannot cross H_1 once they enter inside it. It is also observed that the interior equilibrium E_4 lies inside the box H_1. Moreover, E_4 is the only attractor inside H_1, which is established in the following theorem. □

Uniform persistence

Definition A population F(t) is said to be uniformly persistent if there exist constants $0<\alpha<\beta<\infty$ such that $\alpha \leq \liminf_{t\to\infty} F(t) \leq \limsup_{t\to\infty} F(t) \leq \beta$ for any $F(t)$ with $F(0) > 0$.

Theorem 2 *For model governed by the Eqs.* (1–4)*, fish population F(t) will be Uniformly persistent if* $r_0 > r_1C_0 + \beta$ *and* $K_0 > K_{11}N_u$ (He and Wang 2007, 2009).

Proof From Eq. (1) of the model we have

$\frac{dF}{dt} = R(C)F - \frac{r_0F^2}{K(N)}$.

By the boundedness of the system we obtain that, $F(t) \leq \frac{MK_0}{r_0}$.

Hence,

$$\limsup_{t\to\infty} F(t) \leq \frac{MK_0}{r_0}, \tag{14}$$

then for any given $\epsilon_1 > 0$ $\exists$ $t_1 > 0$ such that $F(t) < \frac{MK_0}{r_0} + \epsilon_1$ for $t > t_1$ and $N(t) < \frac{d_1-a}{g} + \epsilon_1$ for $t > t_1$

$$\frac{dF}{dt} = (r_0 + r_1(C - C_0))F - \frac{r_0F^2}{K_0 - K_{11}N},$$

$$\frac{dF}{dt} \geq (r_0 - r_1C_0)F - \frac{r_0F^2}{K_0 - K_{11}(N_u + \epsilon_1)},$$

$$\frac{dF}{dt} \geq F\left((r_0 - r_1C_0) - \frac{r_0F}{K_0 - K_{11}(N_u + \epsilon_1)}\right). \tag{15}$$

Let $\frac{r_0}{K_0 - K_{11}N_u} = Z > 0$. Where, $K_0 - K_{11}(N_u + \epsilon_1) > 0$ and $r_0 - r_1C_0 > \beta > 0$. where, β and Z are positive constants. Then from inequality (15) we obtain

$$\frac{dF}{dt} \geq F(\beta - ZF),$$

$$\frac{dF}{F(\beta - ZF)} \geq dt,$$

on solving above eqn. we get,

$$F \geq \frac{\beta F_0}{ZF_0 + (\beta - ZF_0)exp(-\beta t)}.$$

Hence,

$$\liminf_{t\to\infty} F(t) \geq \frac{\beta}{Z} > 0. \tag{16}$$

On using the relations (14) and (16), it can be shown with the help of Theorem 1 and positivity of the solutions of the system (1–4) that

$$\frac{\beta}{Z} \leq \liminf_{t\to\infty} F(t) \leq \limsup_{t\to\infty} F(t) \leq \frac{MK_0}{r_0}. \tag{17}$$

Hence, it is proved from relation (17) that the fish population $F(t)$ is uniformly persistent. □

Dynamical behaviour of the model

Local stability analysis

In the previous section, we have found that the model described by Eqs. (1–4) have four equilibria, namely, E_1, E_2, E_3, E_4. Now we will study the dynamical behaviour of the model about four feasible equilibria.

The variational matrix for the system of Eqs. (1–4) evaluated at E_1 is:

$$M_1 = \begin{bmatrix} r_0 + r_1(C^* - C_0) & 0 & 0 & 0 \\ 0 & -K_{20} & 0 & -d_{B1} - K_{20}(C_s - C^*) \\ 0 & 0 & -r & \beta_1 a - \frac{d_1P^*}{b+P^*} \\ 0 & 0 & 0 & \frac{d_1P^*}{b+P^*} - a \end{bmatrix}$$

The eigenvalues of the characteristic equation of the matrix M_1 are $\lambda_1 = r_0 + r_1(C^* - C_0), \lambda_2 = -K_{20}, \lambda_3 = -r, \lambda_4 = \frac{d_1P^*}{b+P^*} - a$. It is noted from these eigenvalues that the equilibrium E_1 is locally asymptotically stable if $r_0 + r_1C^* < r_1C_0$ and $(d_1 - a)P^* < ab$ otherwise E_1 will be unstable.

The variational matrix for the system of Eqs. (1–4) evaluated at E_2 is:

$$M_2 = \begin{bmatrix} -\frac{r_0\hat{F}}{K_0} & r_1\hat{F} & 0 & -\frac{r_0\hat{F}^2K_{11}}{K_0^2} \\ 0 & -K_{20} & 0 & -d_{B1} - K_{20}(C_s - \hat{C}) \\ 0 & 0 & -r & \beta_1 a - \frac{d_1\hat{P}}{b+\hat{P}} \\ 0 & 0 & 0 & \frac{d_1\hat{P}}{b+\hat{P}} - a \end{bmatrix}$$

The eigenvalues of the characteristic equation of the matrix M_2 are $\lambda_1 = -\frac{r_0\hat{F}}{K_0}, \lambda_2 = -K_{20}, \lambda_3 = -r, \lambda_4 = \frac{d_1\hat{P}}{b+\hat{P}} - a.$

It is observed from these eigenvalues that the equilibrium E_2 is locally asymptotically stable if $(d_1 - a)\hat{P} < ab$ otherwise E_2 will be unstable.

The variational matrix for the system of Eqs. (1–4) evaluated at E_3 is:

$$M_3 = \begin{bmatrix} r_0 + r_1(\tilde{C} - C_0) & 0 & 0 & 0 \\ 0 & -\frac{K_{20}}{1+\tilde{N}} & 0 & -d_{B1} - \frac{K_{20}(C_s - \tilde{C})}{(1+\tilde{N})^2} \\ 0 & 0 & -r - \frac{d_1\tilde{N}b}{(b+\tilde{P})^2} & \beta_1 a - \frac{d_1\tilde{P}}{b+\tilde{P}} \\ 0 & 0 & \frac{d_1\tilde{N}b}{(b+\tilde{P})^2} & -g\tilde{N} \end{bmatrix}$$

Two eigenvalues of the characteristic equation of the matrix M_3 are $\lambda_1 = r_0 + r_1(\tilde{C} - C_0), \lambda_2 = -\frac{K_{20}}{1+\tilde{N}}$ and other two eigenvalues λ_3, λ_4 are obtained from the roots of the following quadratic equation i.e.

$$\lambda^2 + \lambda\left(r + \frac{d_1\tilde{N}b}{(b+\tilde{P})^2} + g\tilde{N}\right) + \left(\frac{d_1^2 b\tilde{N}\tilde{P}}{(b+\tilde{P})^3} - \frac{d_1 b\beta_1 a\tilde{N}}{(b+\tilde{P})^2} + rg\tilde{N} + \frac{d_1 bg\tilde{N}^2}{(b+\tilde{P})^2}\right) = 0. \tag{18}$$

Clearly, λ_3, λ_4 have negative real parts if $g\tilde{N} > \beta_1 a$.

Therefore, it is noted from these eigenvalues that the equilibrium E_3 is locally asymptotically stable if $g\tilde{N} > \beta_1 a$ and $r_0 + r_1\tilde{C} < r_1 C_0$ otherwise E_3 will be unstable.

The variational matrix for the system of Eqs. (1–4) evaluated at E_4 is:

$$M_4 = \begin{bmatrix} -\frac{r_0\bar{F}}{K(\bar{N})} & r_1\bar{F} & 0 & -\frac{r_0\bar{F}^2 K_{11}}{K(\bar{N})^2} \\ 0 & -\frac{K_{20}}{(1+\bar{N})} & 0 & -d_{B1} - \frac{K_{20}(C_s - \bar{C})}{(1+\bar{N})^2} \\ 0 & 0 & -r - \frac{d_1\bar{N}b}{(b+\bar{P})^2} & \beta_1 a - \frac{d_1\bar{P}}{b+\bar{P}} \\ 0 & 0 & \frac{d_1\bar{N}b}{(b+\bar{P})^2} & -g\bar{N} \end{bmatrix}$$

Two eigenvalues of the characteristic equation of the matrix M_4 are

$\lambda_1 = -\frac{r_0\bar{F}}{K(\bar{N})}, \lambda_2 = -\frac{K_{20}}{(1+\bar{N})}$ and other two eigenvalues λ_3, λ_4 are the roots of the following quadratic equation

$$\lambda^2 + \lambda\left(r + \frac{d_1\bar{N}b}{(b+\bar{P})^2} + g\bar{N}\right) + \left(\frac{d_1^2 b\bar{N}\bar{P}}{(b+\bar{P})^3} - \frac{d_1 b\beta_1 a\bar{N}}{(b+\bar{P})^2} + rg\bar{N} + \frac{d_1 bg\bar{N}^2}{(b+\bar{P})^2}\right) = 0. \tag{19}$$

Thus, it is noted from these eigenvalues that the equilibrium E_4 is locally asymptotically stable if eigenvalues λ_3, λ_4 have negative real parts. Clearly λ_3, λ_4 have negative real parts if $g\bar{N} > \beta_1 a$.

Global stability analysis of the interior equilibrium point

Theorem 3 *The interior equilibrium $E_4 \in H_1 \subset R_+^4$ is globally asymptotically stable if following inequalities hold:*

$$\left(\frac{r_0}{K_0 - K_{11}N_l}\right)\left(\frac{K_{20}}{1+N_u}\right) > r_1^2, \tag{20}$$

$$\frac{2}{3}\left(\frac{r_0}{K_0 - K_{11}N_l}\right)g > \left(\frac{r_0\bar{F}K_{11}}{(K_0 - K_{11}N_u)(K_0 - K_{11}\bar{N})}\right)^2, \tag{21}$$

$$\frac{2}{3}\left(\frac{K_{20}}{1+N_u}\right)g > \left(d_{B1} + \frac{K_{20}}{(1+N_l)(1+\bar{N})}(C_s - \bar{C})\right)^2, \tag{22}$$

$$\frac{4}{3}\left(r + \frac{d_1 N_l b}{(b+P_u)(b+\bar{P})}\right)g > \left(\beta_1 a - \frac{d_1\bar{P}}{b+\bar{P}} + \frac{d_1 b}{(b+P_l)(b+\bar{P})}\right)^2. \tag{23}$$

Proof Let us consider a positive definite function:

$$W(F,C,P,N) = (F - \bar{F} - \bar{F}ln\frac{F}{\bar{F}}) + \frac{1}{2}(C - \bar{C})^2 + \frac{1}{2}(P - \bar{P})^2 + (N - \bar{N} - \bar{N}ln\frac{N}{\bar{N}}). \tag{24}$$

On differentiating W given by (24) with respect to time t, we get

$$\frac{dW}{dt} = \frac{dW_1}{dt} + \frac{dW_2}{dt} + \frac{dW_3}{dt} + \frac{dW_4}{dt}, \tag{25}$$

where,

$$\frac{dW_1}{dt} = \{r_1(C - \bar{C})(F - \bar{F}) - \frac{r_0\bar{F}K_{11}}{(K_0 - K_{11}N)(K_0 - K_{11}\bar{N})}(N - \bar{N})(F - \bar{F}) - \frac{r_0}{K_0 - K_{11}N}(F - \bar{F})^2\},$$

$$\frac{dW_2}{dt} = \{-\frac{K_{20}}{1+N}(C - \bar{C})^2 - \left(d_{B1} + \frac{K_{20}}{(1+N)(1+\bar{N})}(C_s - \bar{C})\right)(N - \bar{N})(C - \bar{C})\},$$

$$\frac{dW_3}{dt} = -\left(r + \frac{d_1 Nb}{(b+P)(b+\bar{P})}\right)(P - \bar{P})^2 + \left(\beta_1 a - \frac{d_1\bar{P}}{b+\bar{P}}\right)(N - \bar{N})(P - \bar{P})\Bigg\},$$

$$\frac{dW_4}{dt} = \left\{ -g(N-\bar{N})^2 + \frac{d_1 b}{(b+P)(b+\bar{P})}(N-\bar{N})(P-\bar{P}) \right\}.$$

On substituting the values of $\frac{dW_1}{dt}, \frac{dW_2}{dt}, \frac{dW_3}{dt}, \frac{dW_4}{dt}$ in eqn. (25), we get the following expression in region H_1

$$\begin{aligned}\frac{dW}{dt} = &-\{a_{11}(F-\bar{F})^2 + a_{22}(C-\bar{C})^2 + a_{33}(P-\bar{P})^2 + a_{44}(N-\bar{N})^2 \\ &- a_{12}(C-\bar{C})(F-\bar{F}) + a_{14}(N-\bar{N})(F-\bar{F}) + a_{24}(N-\bar{N})(C-\bar{C}) \\ &- a_{34}(N-\bar{N})(P-\bar{P})\}\end{aligned} \tag{26}$$

where,

$$a_{11} = \frac{r_0}{K_0 - K_{11}N}, \qquad a_{22} = \frac{K_{20}}{1+N},$$

$$a_{33} = \left(r + \frac{d_1 N b}{(b+P)(b+\bar{P})} \right), \qquad a_{44} = g,$$

$$a_{12} = r_1, \qquad a_{14} = \frac{r_0 \bar{F} K_{11}}{(K_0 - K_{11}N)(K_0 - K_{11}\bar{N})},$$

$$a_{24} = \left(d_{B1} + \frac{K_{20}}{(1+N)(1+\bar{N})}(C_s - \bar{C}) \right), \qquad a_{34} = \left(\beta_1 a - \frac{d_1 \bar{P}}{b+\bar{P}} + \frac{d_1 b}{(b+P)(b+\bar{P})} \right)$$

The stability region H_1 is given by: $\{H_1 = (F, C, P, N) \in R_+^4 : 0 \le F \le 1.3274, 0 \le C \le 318.5104, 0.1454 \le P \le 75.0413, 10.0597 \le N \le 16.6852\}$.

From the simulation analysis it is noted that the conditions for the stability of equilibrium point E_4 are satisfied in the region H_1 proving that E_4 is asymptotically stable for the above set of parameters (see Fig. 1).

Further, to illustrate the global stability of interior equilibrium E_4 of the model graphically, numerical simulation is performed for the above set of parameters with different initial conditions (see Tables 1, 2, 3) and respective phase plane graphs for F–C, C–P and C–N are shown in Figs. 2, 3, 4. These figures illustrate that all the trajectories starting from different initial conditions reach to the interior equilibrium E_4 as time elapses demonstrating the global stability.

In order to investigate the effect of I on the dynamics of N, C, and F, we further perform numerical simulation and plot the graphs with respect to time (see Figs. 5, 6, 7).

The boundary equilibrium point $E_1(0, 3.0025, 0.1667, 0)$ of the system is locally asymptotically stable (see Fig. 8) for the following set of parameters: $r_0 = 0.1, r_1 = 0.05, K_0 = 0.2, K_{11} = 0.04, d_{B0} = 8, d_{B1} = 0.001, K_{20} = 2, \beta_1 = 0.01, C_s = 7, I = 1, r = 6, d_1 = 0.5, b = 0.6, a = 0.4, C_0 = 6, g = 0.9, N_0 = 5$.

The boundary equilibrium point $E_2(1.2000, 3.0025, 0.1667, 0)$ of the system is locally asymptotically stable (see Fig. 9) for the following set of parameters: $r_0 = 2.0, r_1 = 0.001, K_0 = 1.2, K_{11} = 0.04, d_{B0} = 8, d_{B1} = 0.001, K_{20} = 2, \beta_1 = 0.01, C_s = 7, I = 1.0, r = 6, d_1 = 0.5, b = 0.8, a = 0.4, C_0 = 3, g = 0.9, N_0 = 5.0$.

The boundary equilibrium point $E_3(0, 0.7584, 38.2843, 16.6417)$ of the system is locally asymptotically stable (see Fig. 10) for the following set of parameters: $r_0 = 0.33, r_1 = 0.05, K_0 = 2.5, K_{11} = 0.05, d_{B0} = 9.8, d_{B1} = 0.008, K_{20} = 10, \beta_1 = 0.01, C_s = 18, I = 31.9, r = 0.4, d_1 = 1.0, b = 0.09, a = 0.099, C_0 = 17, g = 0.054, N_0 = 20$. Figs. 8,9, 10 shows the stable behavior of the trajectories of the model for equilibrium points E_1, E_2 and E_3.

Using Sylvester's criteria we obtained the following sufficient conditions for $\frac{dW}{dt}$ to be negative definite

$$(i) a_{11}a_{22} > a_{12}^2, (ii) \frac{2}{3}a_{11}a_{44} > a_{14}^2, \tag{27}$$

$$(iii) \frac{2}{3}a_{22}a_{44} > a_{24}^2, (iv) \frac{4}{3}a_{33}a_{44} > a_{34}^2 \tag{28}$$

We note that the conditions (20–23) implies inequalities obtained in (27) and (28) after using region of attraction. Therefore,by Lyapunov's direct method we find that E_4 is globally (nonlinearly) asymptotically stable in the region H_1. □

Numerical simulation

In this section, we present a numerical simulation to support the applicability of analytical results by choosing the following values of the parameters in model given by Eqs. (1–4).

$r_0 = 3, r_1 = 0.001, K_0 = 1.2, K_{11} = 0.06, d_{B0} = 7, d_{B1} = 0.005, K_{20} = 10, \beta_1 = 0.01, C_s = 18, I = 30, r = 0.4, d_1 = 1.0, b = 0.081, a = 0.099, C_0 = 5, g = 0.054, N_0 = 20$.

Under the above set of parameters, it is shown that the conditions for the existence of interior equilibrium $E_4(\bar{F}, \bar{C}, \bar{P}, \bar{N})$ are satisfied and the equilibrium values are $\bar{F} = 0.2016, \bar{C} = 5.6812, \bar{P} = 33.5400, \bar{N} = 16.6406$.

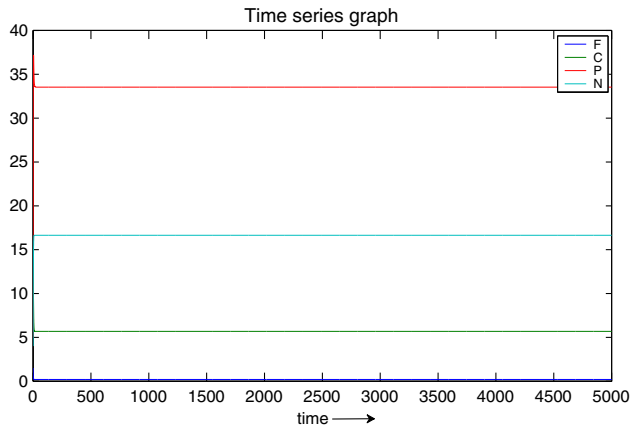

Fig. 1 Trajectories of the model with respect to time with initial values (1.5, 15, 5, 4) showing stability behavior

Table 1 Different initial conditions for F and C of the model

F	0.08	0.1	0.4	0.5	0.6
C	7.5	3.2	6.5	4	8.1

Table 2 Different initial conditions for C and P of the model

C	2	3	8	11	13
P	36	29	28	31	34

Table 3 Different initial conditions for C and N of the model

C	3	5	8	8.5
N	17.5	12	19	15

Conclusion

In this paper, we have proposed and analyzed a nonlinear mathematical model to study the effect of increasing algal biomass due to nutrient overloading on the concentration of dissolved oxygen and the survival of fish population in an aquatic ecosystem. The local and global stability analysis of the equilibrium points of the model is carried out. From the stability analysis of boundary equilibrium point E_1 and E_3 it is noted that the fish population tend to extinction due to decrease in the concentration of dissolved oxygen from its threshold level. The stability analysis of boundary equilibrium point E_2 shows that the fish population survive because in this case concentration of dissolved oxygen is more than its threshold level. From the stability analysis of interior equilibrium point E_4 it is observed that the fish population will survive at very low equilibrium level due to reduced concentration of dissolved oxygen and excessive presence of algal biomass on account of nutrient loading.

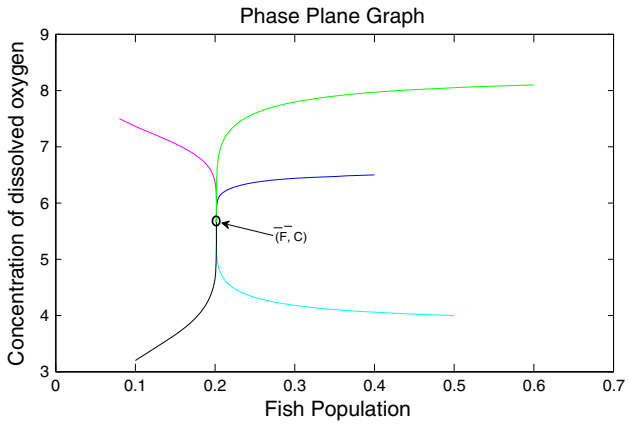

Fig. 2 Global stability in F–C plane

These stability results are depicted in the Figs. 1–17 using numerical simulation. From Fig. 5 it is shown that as the input rate of nutrients I increases then the algal biomass increases. Figure 6 shows that as the input rate of nutrients I increases then the concentration of dissolved oxygen decreases with respect to time. Figure 7 shows the dynamics of fish population for different values of I i.e. input rate of nutrients (phosphorus and nitrogen) with respect to time. From this fig. it is observed that the density of fish population decreases as the input concentration of nutrients increases illustrating the role of nutrient overloading on fish population. Thus, it is concluded here that if the nutrients are excess in amount than the required level then the survival of fish population is threatened. These numerical results suggest the role of nutrient loading on the fate of dissolved oxygen and consequently on the growth dynamics of algal biomass and fish population. The variation in fish population with respect to the concentration of dissolved oxygen for different initial conditions are shown in Figs. 11 and 12. From Fig. 11 it is clear that when the concentration of dissolved oxygen decreases then fish population also decreases. From Fig. 12 we observe that as the concentration of dissolved oxygen increases then the fish population increases slowly but as the concentration of dissolved oxygen approaches to the saturated level, fish population continues to increase and then after some time concentration of dissolved oxygen and fish population both starts decreasing simultaneously due to the onset of algal bloom. Figure 13 shows the variation in algal biomass with respect to the concentration of nutrients (phosphorus and nitrogen) and from this we observe that as the concentration of nutrient increases then the algal biomass increases. Figure 14 shows that as the concentration of nutrients increases then the concentration of dissolved oxygen decreases establishing the analytical result. The variation in fish population with respect to the concentration of nutrients (phosphorus and nitrogen) is shown in Fig. 15. From

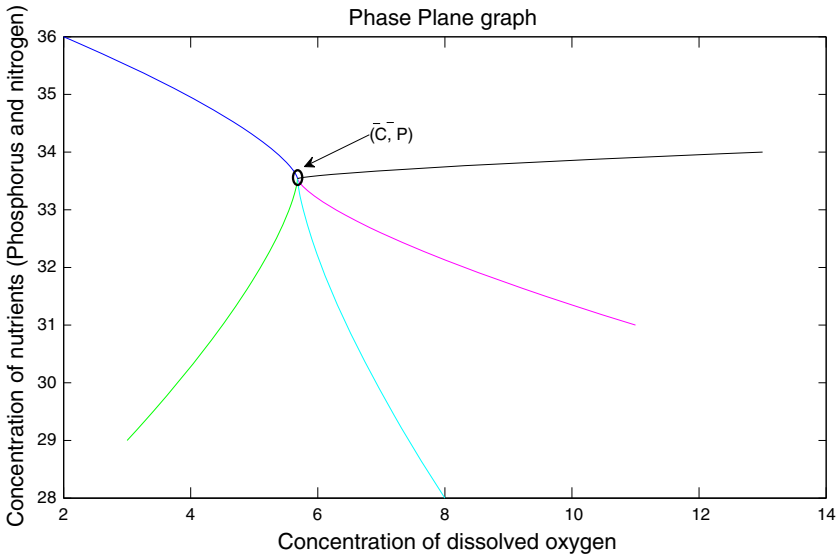

Fig. 3 Global stability in C–P plane

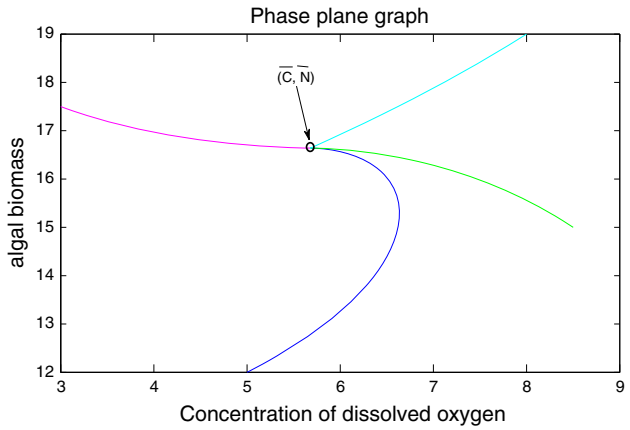

Fig. 4 Global stability in C–N plane

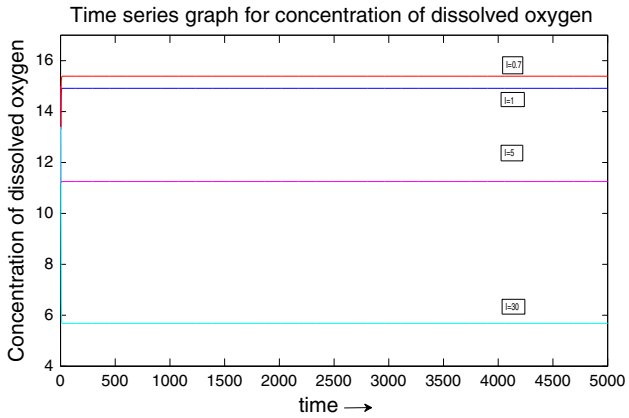

Fig. 6 Stable interior equilibrium concentration of dissolved oxygen (C) for different values of I

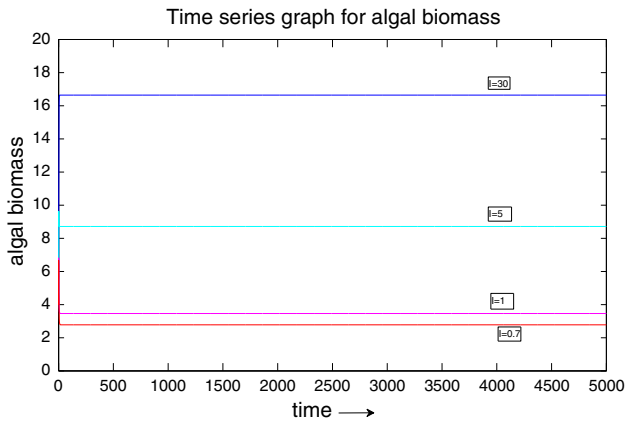

Fig. 5 Stable interior equilibrium level of algal biomass for different values of I

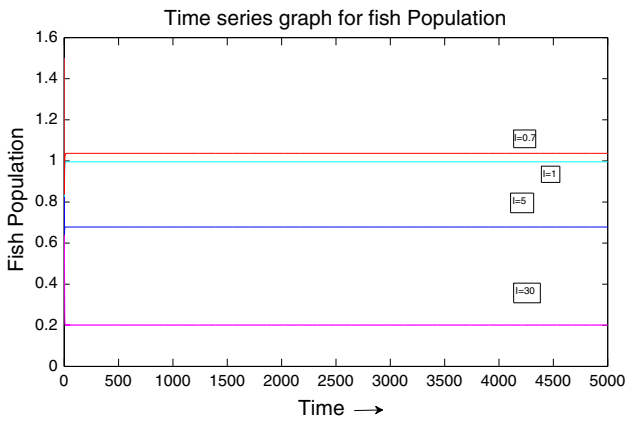

Fig. 7 Stable interior equilibrium fish population (F) for different values of I

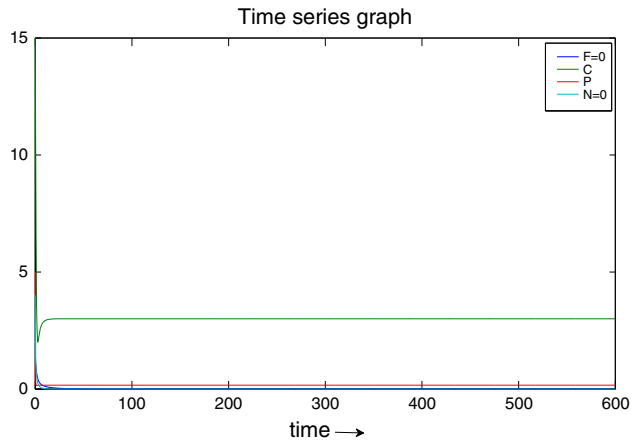

Fig. 8 The boundary equilibrium point E_1 where $F = 0$ and $N = 0$ is asymptotically stable

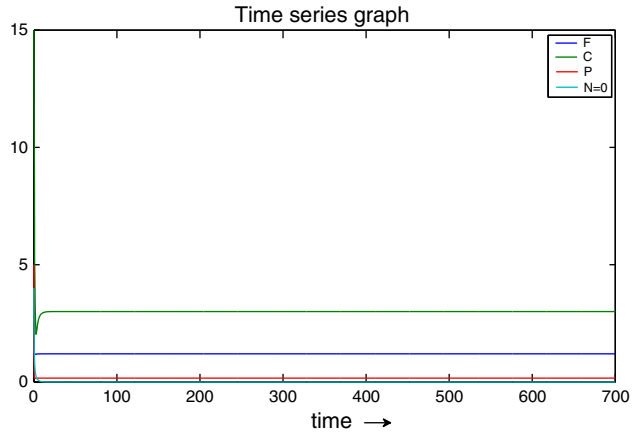

Fig. 9 The boundary equilibrium point E_2 where $N = 0$ is asymptotically stable

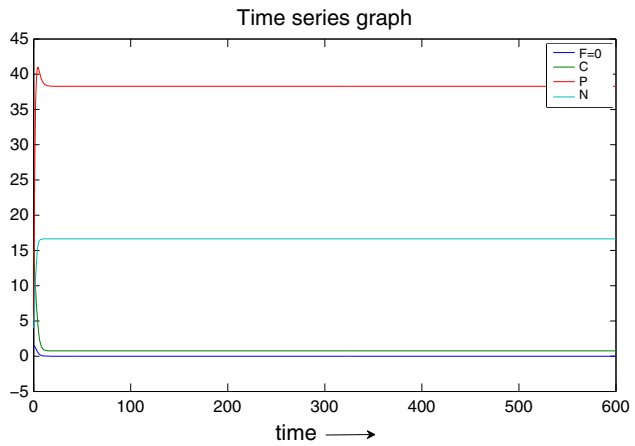

Fig. 10 The boundary equilibrium point E_3 where $F = 0$ is asymptotically stable

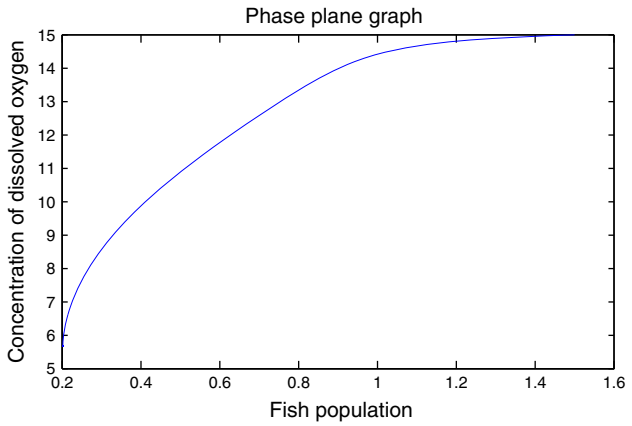

Fig. 11 Phase plane plot between fish population (F) and concentration of dissolved oxygen (C) with initial values: $F(0) = 1.5$, $C(0) = 15$ in the case of interior equilibrium point

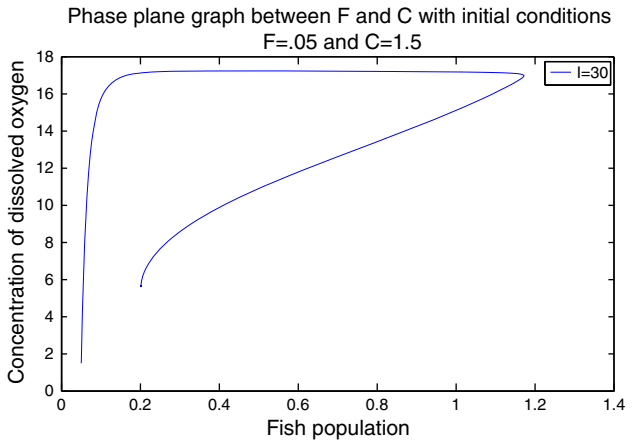

Fig. 12 Phase plane plot between fish population (F) and concentration of dissolved oxygen (C) with initial values: $F(0) = 0.05$, $C(0) = 1.5$ in the case of interior equilibrium point

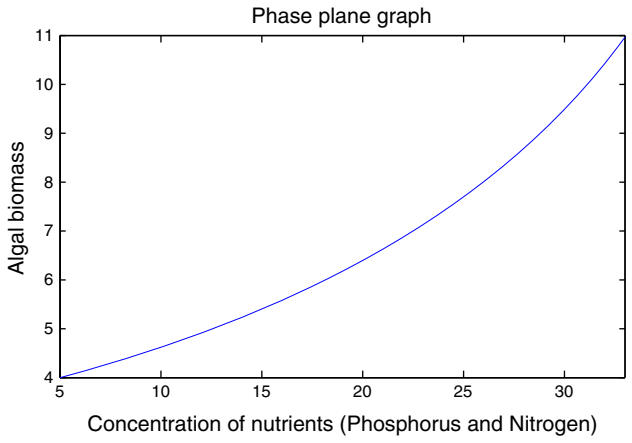

Fig. 13 Phase plane plot between concentration of nutrients (phosphorus and nitrogen) (P) and algal biomass (N) with initial values: $P(0) = 5$, $N(0) = 4$ in the case of interior equilibrium point

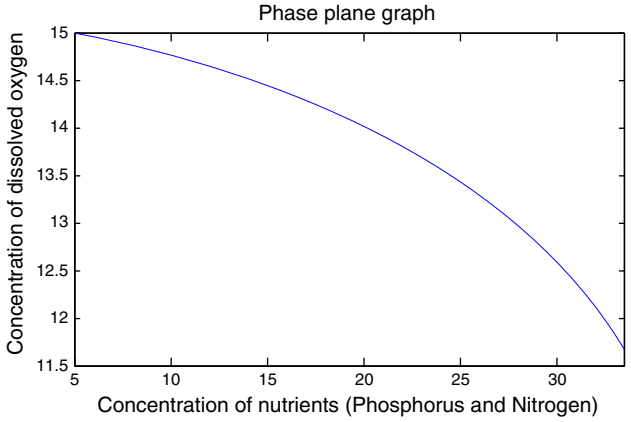

Fig. 14 Phase plane plot between concentration of dissolved oxygen (C) and concentration of nutrients (phosphorus and nitrogen) (P) with initial values: C(0) = 15, P(0) = 5 in the case of interior equilibrium point

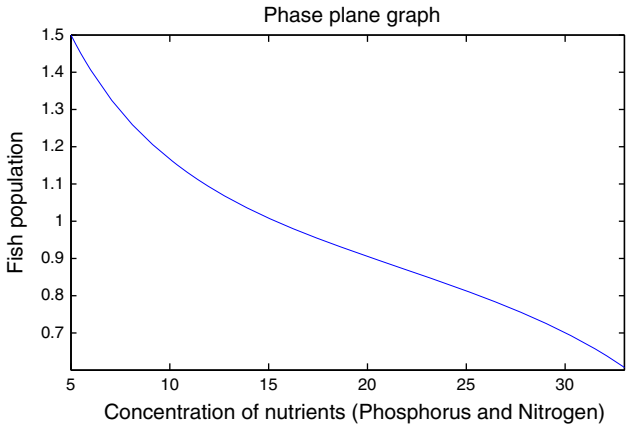

Fig. 15 Phase plane plot between concentration of nutrients (phosphorus and nitrogen) (P) and fish population (F) with initial values: P(0) = 5, $F(0) = 1.5$ in the case of interior equilibrium point

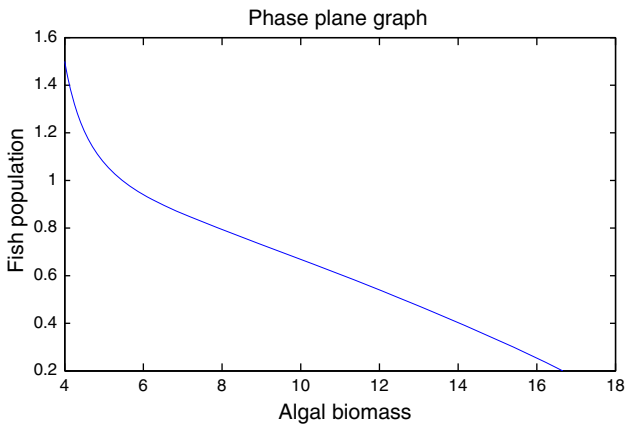

Fig. 16 Phase plane plot between algal biomass and fish population (F) with initial values: $N(0) = 4, F(0) = 1.5$ in the case of interior equilibrium point

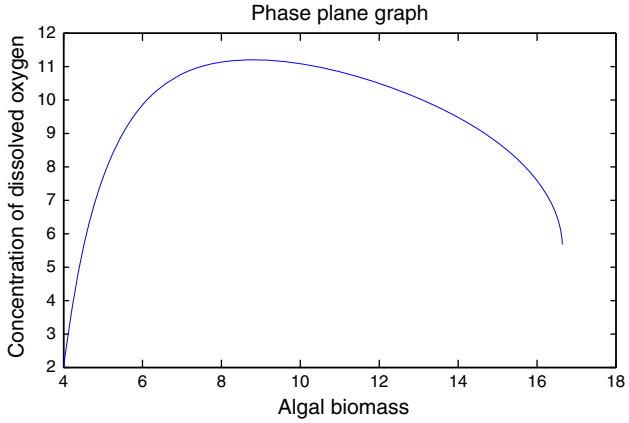

Fig. 17 Phase plane plot between algal biomass (N) and concentration of dissolved oxygen (C) with initial values: N(0) = 4, C(0) = 2 in the case of interior equilibrium point. The phase plane trajectory shown in this graph is qualitatively similar to the behaviour as shown graphically (fig. 1) in the paper by Smith and Piedrahita (1988)

this figure it is noted that as the concentration of nutrients (phosphorus and nitrogen) increases, the fish population decreases on account of reduced equilibrium level of dissolved oxygen. In Fig. 16 it is shown that the fish population decreases when the algal biomass increases due to excessive nutrient concentration. Figure 17 shows the variation in concentration of dissolved oxygen with respect to algal biomass. This figure shows that the concentration of dissolved oxygen initially increases with the increase in the density of algae but when the algal biomass is more than what the aquatic ecosystem can handle then the dissolved oxygen concentration starts decreasing (see fig. 1 in the paper of Smith and Piedrahita 1988).

References

Anderson DM, Glibert PM, Burkholder JM (2002) Harmful algal blooms and eutrophication: nutrient source, composition and consequences. Estuar Res Fed 25(4b):704–726

Alvarez-Vazquez LJ, Fernandez FJ, Munoz-Sola R (2009) Mathematical analysis of a three-dimensional eutrophication model. J Math Anal Appl 349:135–155

Chau KW (2004) A three-dimensional eutrophication modeling in Tolo Harbour. Appl Math Modell 28:849–861

Camargo JA, Alonso A (2006) Ecological and toxicological effects of inorganic nitrogen pollution in aquatic ecosystems: a global assessment. Environ Int 32:831–849

Chen S, Chen X, Peng Y, Peng K (2009) A mathematical model of the effect of nitrogen and phosphorus on the growth of blue-green algae population. Appl Math Modell 33:1097–1106

Chakraborty K, Das K (2015) Modeling and analysis of a two-zooplankton one-phytoplankton system in the presence of toxicity. Appl Math Modell 39:1241–1265

Chakraborty Subhendu, Tiwari PK, Misra AK, Chattopadhyay J (2015) Spatial dynamics of a nutrient-phytoplankton system with toxic effect on phytoplankton. Math Biosci 264:94–100

Huppert Amit, Blasius Bernd, Stone Lewi (2002) A Model of Phytoplankton Blooms. Am Soc Nat 159:156–171

Huppert Amit, Blasius Bernd, Olinky Ronen, Stone Lewi (2005) A model for seasonal phytoplankton blooms. J Theor Biol 236:276–290

He J, Wang K (2007) The survival analysis for a single-species population model in a polluted environment. Appl Math Modell 31:2227–2238

He J, Wang K (2009) The survival analysis for a population in a polluted environment. Nonlinear Anal Real World Appl 10:1555–1571

Hale JK (1969) Ordinary differential equations. Wiley Interscience, NY

Misra AK, Chandra P, Shukla JB (2006) Mathematical modeling and analysis of the depletion of dissolved oxygen in water bodies . Nonlinear Anal Real World Appl 7:980–996

Misra AK (2011) Modeling the depletion of dissolved oxygen due to algal bloom in a lake by taking Holling type-III interaction. Applied Mathematics and Computation 217:8367–8376

Reynolds CS (1991) Toxic blue-green algae: the problem in perspective. Freshw Biol Assoc 1:29–38

Smith DW, Piedrahita RH (1988) The relation between phytoplankton and dissolved oxygen in fish Ponds. Aquaculture 68:249–265

Shukla JB, Misra AK, Chandra P (2007) Mathematical modeling of the survival of a biological species in polluted water bodies. Differ Equ Dyn Syst 15(3):209–230

Shukla JB, Misra AK, Chandra P (2008) Mathematical modeling and analysis of the depletion of dissolved oxygen in eutrophied water bodies affected by organic pollutants. Nonlinear Anal Real World Appl 9:1851–1865

Walker WW Jr, Havens KE (1995) Relating algal bloom frequencies to phosphorus concentrations in lake Okeechobee. Lake Reserv Manag 11(1):77–83